CFSRC COLLOQUIUM

Proceedings of the Cold-Formed Steel Research Consortium Colloquium
17-19 October 2022 (cfsrc.org)

Innovative concrete-filled cold-formed steel (CF-CFS) built-up columns

Rohola Rahnavard[1], Hélder D. Craveiro[2], Rui A. Simões[3]

Abstract

This paper presents an innovative type of concrete-filled cold-formed steel (CF-CFS) built-up composite column. Twenty-four innovative specimens of four CF-CFS cross-section configurations were used to investigate their behavior at ambient and elevated temperatures. First, the axial load-bearing capacity of the innovative CF-CFS was obtained using a series of experimental tests under pure compression. Then their fire resistance was evaluated using another series of experimental tests subjected to elevated temperatures. Moreover, finite element modeling approaches were developed to further explore the behavior of the CF-CFS composite columns. The applicability of the available design codes, including EN 1994-1-1 and EN 1994-1-2 for the CF-CFS composite column, was discussed. The results showed that the design codes could conservatively predict the CF-CFS composite columns when the effective cross-sectional area was used to determine the Class 4 CFS components. In contrast, unconservative results were obtained using the gross cross-sectional area. Enhanced design methodologies were developed, tackling the specificities associated with the use of built-up tubular steel sections. Therefore, a modification was introduced for the innovative CF-CFS columns to predict buckling and fire resistance with a good agreement. Reliability analysis was also performed to assess the design methodology further by comparing the reliability index for each methodology.

1. Introduction

CFS built-up members are widely used in the building construction industry, and their versatility leads to continuous evolution in how standard products are used. The CFS built-up members are susceptible to local buckling phenomena, leading to low axial capacity. CFS built-up section filled with concrete can be an option to overcome the early local buckling and result in a higher load-bearing capacity. Moreover, formworks are not required for concrete casting as steel boxes remain in the structure. Moreover, due to its low thermal conductivity and thermal expansion, concrete can play an essential role in a composite column exposed to fire.

Concrete-filled steel tube (CFST) columns have been evaluated using experimental, analytical, and numerical research over the past decades [1-15]. Different design codes [16-17] also provide extensive coverage of the design of CFST columns. A literature review revealed that no research study addressed the performance of CF-CFS built-up composite columns. Moreover, the design codes do not consider thin-walled CFS profiles when developing concrete-filled CFS built-up tubular columns. The present investigation assessed the performance of 24 CF-CFS built-up specimens with four distinct cross-sectional configurations. Two types of test setups, including compression and fire tests, were conducted to investigate the behavior of the CF-CFS built-up column at ambient and elevated temperatures. Finite element models were developed using Abaqus [18], aiming to reproduce the observed experimental results accurately. The primary motivation for this study was to understand more about the buckling and fire resistance of CF-CFS built-up sections. The experimentally determined axial capacity to theoretical estimates derived from the EN 1994-1-1 [16] were compared. The fire resistance of the mentioned columns was compared with analytical results following EN 1994-1-2 [17]. Additionally, a modified method is suggested and checked against the obtained experimental and numerical results.

2. Experimental campaign

The experimental buckling and fire resistance tests were conducted in the structural laboratory within the research unit ISISE, Institute for Sustainability and Innovation in Structural Engineering research unit at the Department of Civil Engineering, University of Coimbra. The tests were part

[1] Ph.D. candidate, University of Coimbra, ISISE, Department of Civil Engineering, Coimbra, Portugal, rahnavard1990@gmail.com; rahnavard@uc.pt
[2] Researcher, University of Coimbra, ISISE, Department of Civil Engineering, Coimbra, Portugal, heldercraveiro.eng@uc.pt
[3] Associate professor, University of Coimbra, ISISE, Department of Civil Engineering, Coimbra, Portugal, rad@dec.uc.pt

of the project entitled INNOCFSCONC - Innovative hybrid structural solutions using cold-formed steel and lightweight concrete [19-23].

2.1 Geometry and material properties

In this investigation, CFS built-up sections were created using the C, U, and Σ-shaped CFS profiles. In Figure 1, the geometry of these profiles can be seen in detail. The S280GD+Z structural steel was used to create all the profiles. Five rows of self-drilling fasteners were used to connect the different CFS profiles to create the built-up CFS sections. Each specimen had a length of 1050 mm. The end distance was 50 mm, while the space between rows of fasteners was 237.5 mm (see Figure 1). The fasteners were 6.3 mm in diameter and 45 mm in length. It is important to note that just about 3 mm of the fastener length is utilized to join the CFS plates, while the remaining 42 mm was immersed in the concrete-filled, which may aid in improving the composite action between the steel and concrete. Lightweight concrete was used to fill all the CFS built-up columns.
The material properties were measured using a set of coupon tests for the CFS [19, 20] and cubic compression tests for lightweight concrete [19, 20]. The modulus of elasticity (E_s), yield strength (f_y), ultimate strength (f_u), and proportional stress limit (f_p) were determined for the S280GD+Z structural steel as 204.18 GPa, 306.81 MPa, 424.04 MPa, and 212.50 MPa, respectively [19, 20]. The mean compressive strength (f_{cm}) and density (D) for the lightweight concrete were obtained as 33 MPa and 1850 kg/m^3, respectively.

2.2 Test setup instrumentation

This study used two types of test setups: compression tests to evaluate the buckling resistance of CF-CFS built-up columns and fire resistance tests to investigate the structural behavior of the CF-CFS built-up columns.

2.2.1 Buckling resistance test

The axially compressive force on the CF-CFS built-up short column specimens was applied using a hydraulic testing machine with a capacity of 5000 kN (Figure 2a). The CF-CFS built-up short columns were set up in the testing machine to ensure the specimens were vertical and in the same position throughout the experiment. Both columns' ends were fixed against translational and rotational movements. A load was applied with the displacement controlled at a constant rate of 0.01 mm/s. The vertical shortening displacement was measured during the test using a 100 mm rage Linear Variable Differential transformer (LVDTs). The CF-CFS built-up column tests were stopped when clear drops of the axial load were observed.

2.2.2 Fire resistance test

The fire resistance test setup is shown in Figure 2b. The serviceability load was applied using a 3000 kN capacity hydraulic jack that was permanently mounted to the reaction frame, while the thermal action was applied using a modular electric furnace. The serviceability load corresponded to 50% of the buckling load obtained from the compression test. Once the desired serviceability load was reached, the furnace was turned on to apply thermal action while the load remained constant (50% of the buckling load) during the fire test.
Column ends were fixed to prevent translational and rotational movements. The top beams of the support frame were free to expand axially. This furnace was programmed to reproduce an environment with temperatures based on the standard fire curve ISO 834 [24]. The thermocouples type K were placed at different height levels to measure the gas temperature inside the furnace. The column in the furnace collapsed due to the increasing temperatures and consequent degradation of the mechanical properties of the structural materials.
An extensive set of thermocouples (type K) were also placed in different locations along the column to measure the temperature at the surface of the column. The concrete's temperature was measured using a thermocouple type K placed inside the concrete.

3. Numerical modeling

Numerical models were developed using the software Abaqus [18] to reproduce the observed experimental behavior, contributing to a better understanding of the CF-CFS built-up columns.

3.1 Buckling resistance modeling

The CFS profiles were modeled using the 4-node shell element type (S4R) available in Abaqus [18]. An 8-node linear brick element (C3D8R) was used for modeling infilled concrete. A 10 mm mesh size was used for the modeling. The fasteners were defined using the combined "beam connector and fastener" approach from the Abaqus library [18]. Previous studies showed that the combined "beam connector and fastener" approach could accurately represent the fasteners' modeling [19, 20]. The interaction between surfaces was considered by defining a friction coefficient of 0.4. Moreover, hard contact was considered to define normal contact.
The mechanical properties of steel were defined as an elastoplastic material. The modulus of elasticity was defined as 204.18 GPa, as mentioned in Section 2.1. The plastic behavior with isotropic hardening was obtained from the true stress-strain curve, which was converted from experimental stress-strain curves [19, 20]. The concrete's modulus of elasticity (E_{cm}) was considered 31.476 GPa according to EN

1992-1-1 [25], corresponding to the mean compressive strength obtained from the cubic tests. The concrete damage plasticity model (CDP) was used to define the plastic properties of concrete. The compressive stress-strain relation was defined using Equation 1 as suggested by EN 1992-1-1 [25], where ε_{c1} is the strain corresponding to the peak stress and is equal to 0.0021.

$$\sigma_c = \frac{(k\eta-\eta^2)f_{cm}}{1+(k-2)\eta};\ \eta = \frac{\varepsilon_c}{\varepsilon_{c1}}\ and\ k = 1.05E_{cm}\frac{\varepsilon_{c1}}{f_{cm}} \quad (1)$$

The tensile stress-strain curve was defined in elastic and plastic terms. The peak value of tensile strength (f_{ctm}) was considered 2.6 MPa based on EN 1992-1-1 [25]. Tensile stress increases linearly along with modulus of elasticity, up to the peak value, then reduces linearly to the cracking strain of 0.001 and tensile stress of 5% of the maximum tensile strength [19, 20].

The models were loaded concentrically under displacement control using the nonlinear dynamic explicit procedure. The displacement was applied using Abaqus's "smooth amplitude" technique to prevent convergence error. According to the literature, the scaling factor was considered for the CFS built-up and lightweight concrete-filled components [18-20]. Note that the scaling factor was selected in a way that the ratio of the kinematic energy to the total strain energy (ALLIE) remained below 1%.

The initial imperfection was defined for the modeling by considering the first buckling mode obtained from an elastic buckling analysis. The amplitude of 1/300 of the column's length based on EN 1994-1-1 [16] was defined.

3.2 Fire resistance modeling

A similar modeling approach was considered for modeling the fire resistance behavior of the CF-CFS built-up composite columns. The same meshing and interaction were considered. The mechanical properties of concrete and steel were defined as temperature dependent. The modulus of elasticity and yield strength at elevated temperature was defined according to the stress-strain curves obtained in [26].

The elastic behavior of concrete was defined by applying a reduction factor for elevated temperatures, as found in [21-23, 26]. Concrete was defined as temperature-dependent material using the CDP model. The compressive and tensile behavior of concrete was defined according to Equations 2 and 3, respectively, presented in EN 1992-1-2 [27]. In Equation 2, $f_{c,\theta}$ and $\varepsilon_{c1,\theta}$ represent the maximum stress and its corresponding strain, varied for different temperatures, and were taken from EN 1992-1-2 [27].

$$\sigma_{c,\theta} = \frac{3\varepsilon f_{c,\theta}}{\varepsilon_{c1,\theta}\left[2+\left(\frac{\varepsilon}{\varepsilon_{c1,\theta}}\right)^3\right]} \quad (2)$$

$$\sigma_{t,\theta} = \begin{Bmatrix} f_{ctm} & 20 \le \theta \le 100 \\ (1-\frac{\theta-100}{500})f_{ctm} & 100 < \theta \le 600 \end{Bmatrix} \quad (3)$$

The nonlinear dynamic explicit was used with the same assumption as Section 3.1 to apply the service load. The initial imperfection was defined the same as explained in Section 3.1. The thermal actions were imported from a separate heat transfer analysis. The heat transfer analysis was performed for each configuration step by step, following [21-23]. Radiation and convection were modeled to represent heat transfer from the fire to the exterior of the sections. The values of 0.23 and 20 W/m^{2}K were used as resultant heat emissivity and convective heat coefficient, respectively [21-23].

4. Experimental and numerical results

4.1 buckling resistance

Figure 3 compares the final failure modes of the experimental specimens and numerical models for the CF-CFS built-up composite columns. As can be seen, the distortional and local buckling modes are visible in the plain external channels (U-shaped profiles) for all columns. Moreover, local buckling for the C-shaped profiles is visible. A good agreement was observed between experimental and numerical models in terms of failure modes.

The axial force vs. shortening displacement curves obtained from the experimental and numerical results are shown in Figure 4. The axial load bearing capacity was obtained from the test results as 737.2 kN, 1014.76 kN, 631.27 kN, and 856.95 kN for R-2C+2U, S-2C+2U, R-2Σ+2U, and S-2Σ+2U, respectively. The results show a close agreement (≤5%) between experimental and numerical results. The Square CF-CFS columns showed relatively higher axial capacities due to the larger concrete area.

4.2 Fire resistance

Figure 5 compares experimental specimens' failure mode and finite element models exposed to fire. In terms of deformation, finite element models and experimental specimens were in close agreement. As can be seen, the local buckling mode was the predominant buckling mode for all CF-CFS built-up columns.

Figure 6 compares the furnace air temperature curves measured during the fire tests and the reference ISO 834 curve. Figure 6 shows that the internal furnace temperature takes longer than expected to meet the ISO 834 fire curve. For the most part, the temperatures in the test furnaces were stable, allowing for reliable comparisons between the fire tests. The results of experimental tests and heat transfer analysis are compared between the CFS surface and infilled concrete in Figure 6. The results show that the heat transfer analysis and the experiments agreed well.

Table 1 compares experimental and numerical data for average steel failure temperature, concrete core failure temperature, and failure time. It is important to note that all thermocouples were used to determine the average temperature of the CFS built-up surfaces. The experimental and numerical results were found to be in good agreement.

Average temperatures from experiments and numerical simulations were compared, leading to a CV of 3.88%. In addition, the average difference in failure time was only 4%. The concrete core temperature was also compared, with a maximum 9% variation found (in the case of S-2Σ+2U).

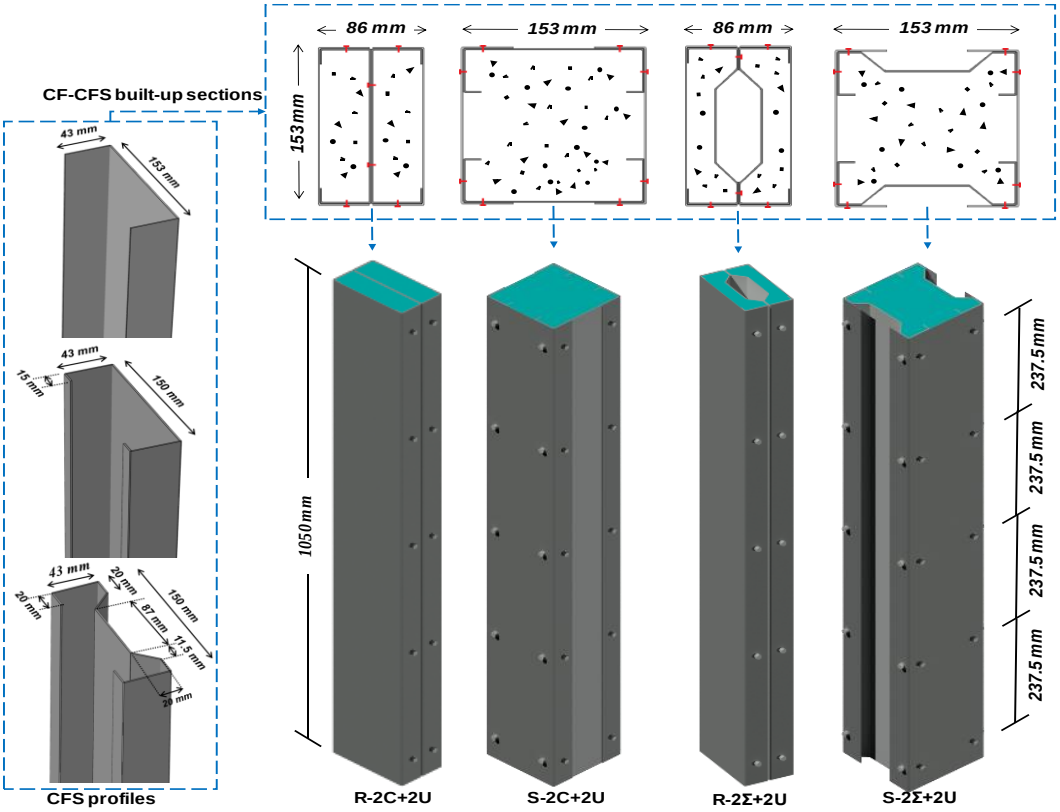

Figure 1: The geometry of the CF-CFS built-up composite columns.

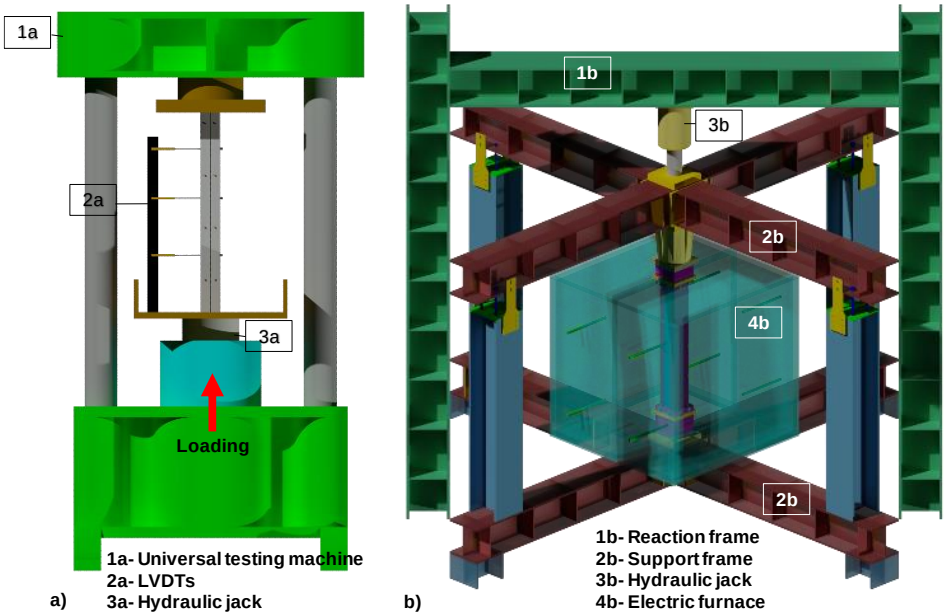

Figure 2: Test setup a) compression test, and b) fire test.

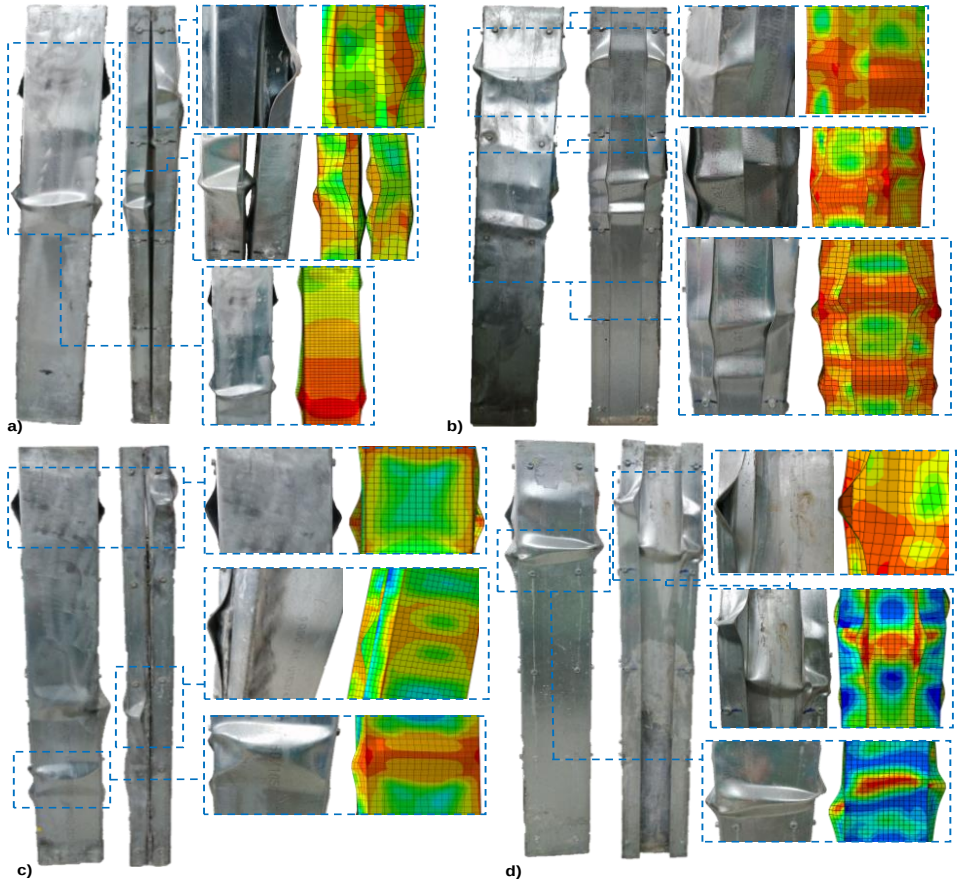

Figure 3: Final deformed shapes for the ambient temperature buckling tests a) R-2C+2U, b) S-2C+2U, c) R-2Σ+2U, and d) S-2Σ+2U.

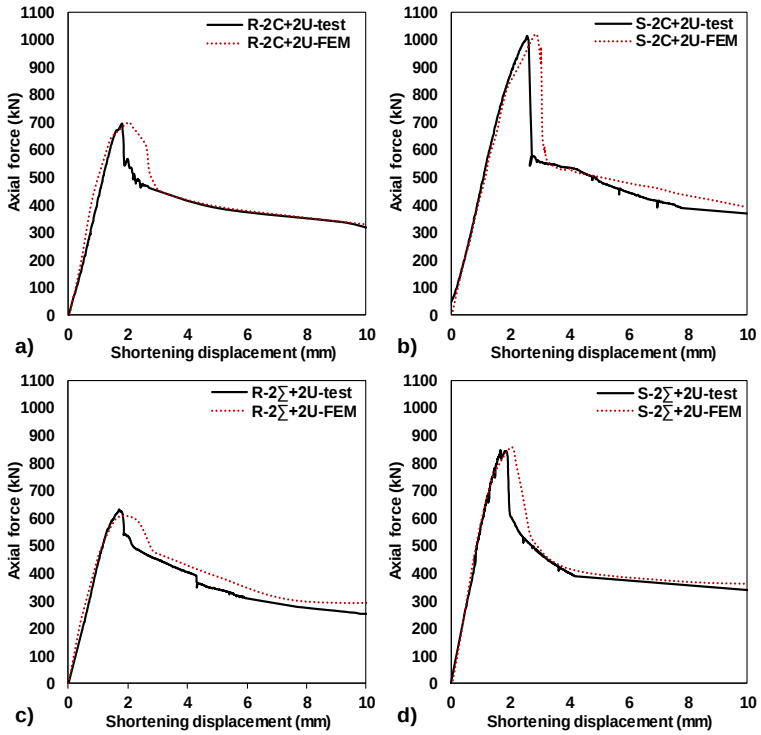

Figure 4: Axial force-displacement a) R-2C+2U, b) S-2C+2U, c) R-2Σ+2U, and d) S-2Σ+2U.

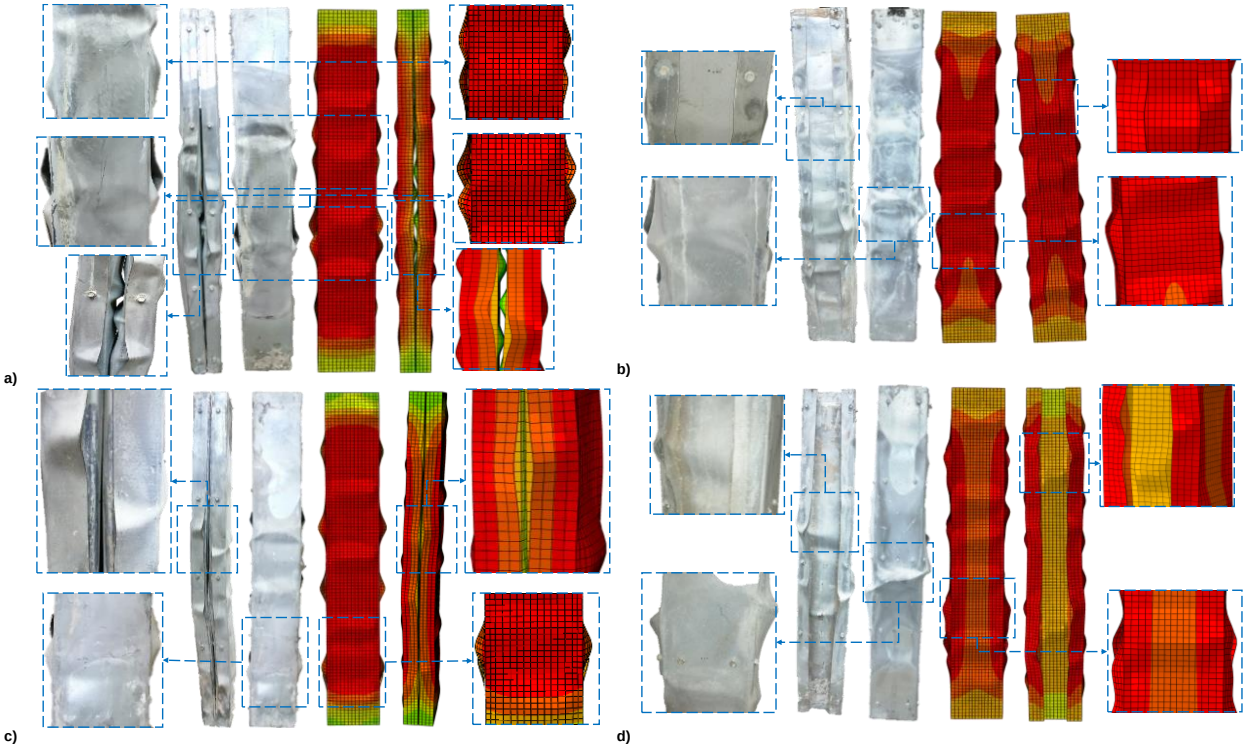

Figure 5: Final failure mode for fire resistance tests a) R-2C+2U, b) S-2C+2U, c) R-2Σ+2U, and d) S-2Σ+2U.

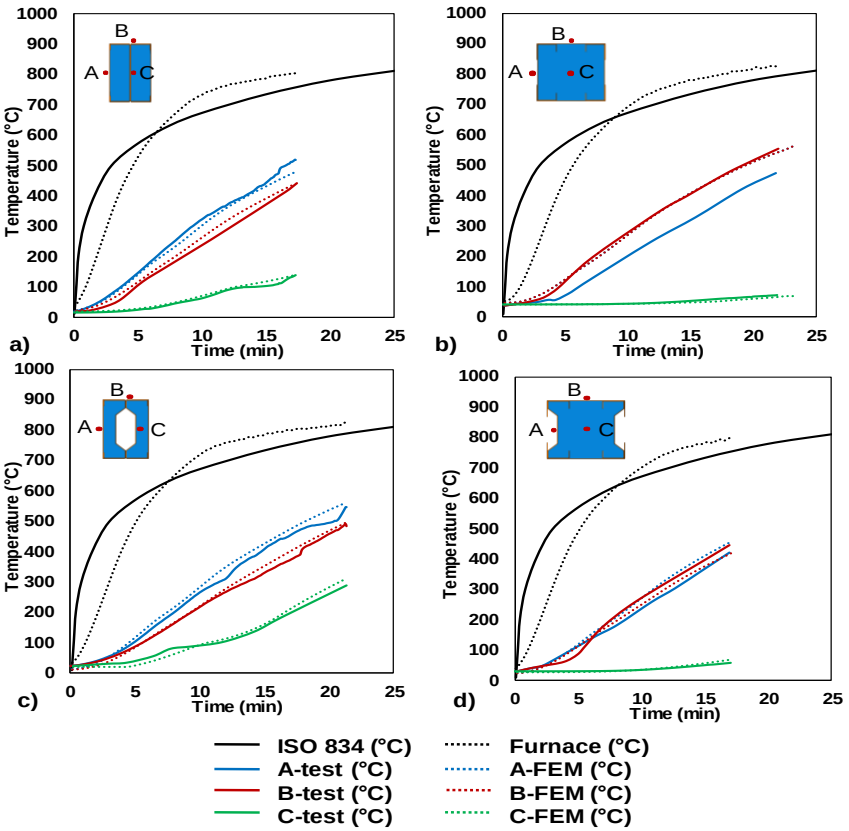

Figure 6: Temperature evolution history a) R-2C+2U, b) S-2C+2U, c) R-2Σ+2U, and d) S-2Σ+2U.

Table 1: Fire resistance tests and model results.

Specimen ID	$\theta_{Failure,s}$ (°C)			$\theta_{Failure,c}$ (°C)			Time (min)		
	EXP	FEM	EXP/FEM	EXP	FEM	EXP/FEM	EXP	FEM	EXP/FEM
R-2C+2U	519.99	508.81	1.02	137.36	138.41	0.99	17.85	18.31	0.97
S-2C+2U	489.86	511.28	0.96	71.13	67.38	1.05	22.10	23.08	0.96
R-2Σ+2U	458.55	451.05	1.02	257.92	249.37	1.03	20.21	19.8	1.02
S-2Σ+2U	475.45	501.22	0.95	72.35	79.49	0.91	16.98	18.98	0.90
m			**0.99**			**1.00**			**0.96**
s			**0.04**			**0.06**			**0.05**
CV (%)			**3.88**			**6.43**			**4.43**

5. Comparison with design predictions

This section compares the buckling and fire resistance of the CF-CFS composite columns obtained from the tests with the analytical methodologies from EN 1994-1-1 [16] and EN 1994-1-2 [17]. Moreover, a modification was introduced for the innovative CF-CFS built-up composite columns to predict buckling and fire resistance. Reliability analysis was also performed following the AISI [28] to assess the design methodologies. The assumption for the reliability analysis can be found in [29]. The reliability index value of 2.5 was considered the target to assess the reliability of the discussed analytical methods [20, 29].

5.1 Buckling resistance according to EN 1994-1-1

The buckling resistance ($N_{b,Rd,1}$) of composite steel-concrete columns can be calculated using Equation 4 following EN 1994-1-1 [16]. In Equation 4, A_a is the gross-cross sectional area of the steel, f_{yd} is the design yield strength of steel, A_c is the concrete section area, f_{cd} is the design value of concrete compressive strength, and χ is the reduction factor due to the column's slenderness.

$$N_{\mathrm{b,Rd},1} = \chi\,(A_a f_{yd} + A_c f_{cd}) \qquad (4)$$

Furthermore, according to EN 1993-1-1 [30], the individual CFS sections employed in this research fell under the category of Class 4 cross-sections. According to EN 1994-1-1 [16], designers must also account for the potential impact of local buckling on resistance. Consequently, the effective areas of the Class 4 cross-sections were calculated using the Effective Width Method (EWM) described in the EN 1993-1-3 [31]. Therefore, another prediction ($N_{\mathrm{b,Rd},2}$) can be based on Equation 5.

$$N_{\mathrm{b,Rd},2} = \chi\,(A_{a,eff} f_{yd} + A_c f_{cd}) \qquad (5)$$

Table 2 lists the analytical and experimental buckling resistance for the CF-CFS built-up composite columns. A detailed analysis of the results shows an unconservative prediction by the current EN 1994-1-1 [16] methodology for CF-CFS built-up composite columns. However, considering the effective area for steel sections shows a conservative prediction. Moreover, the results show a reliability index less than the target value when considering the gross cross-sectional area. The results show that the reliability index (β) is higher than 2.5 for the analytical prediction that used an effective cross-sectional area. Therefore, it can be concluded that the use of EWM leads to a more reliable and safe axial prediction for CF-CFS built-up short columns

Table 2 Comparing the analytical and experimental buckling resistance results.

Specimen ID	P_{EXP} (kN)	$N_{b,Rd,1}$ (kN)	$P_{EXP}/N_{b,Rd,1}$	$N_{b,Rd,2}$ (kN)	$P_{EXP}/N_{b,Rd,2}$
R-2C+2U	737.20	758.65	0.97	557.98	1.32
S-2C+2U	1014.7	998.61	1.01	797.95	1.27
R-2Σ+2U	631.27	695.31	0.90	569.16	1.10
S-2Σ+2U	847.87	930.17	0.91	804.02	1.05
m	-	-	0.95	-	1.18
s	-	-	0.05	-	0.12
CV (%)	-	-	5.45	-	10.7
β	-	-	2.39	-	2.92

5.2 Fire resistance according to EN 1994-1-2

This section discusses the fire resistance for the CF-CFS built-up composite columns. The concrete section is separated into numerous zones of similar thicknesses to determine the fire resistance of a steel-concrete composite column, as specified by EN 1994-1-2 [17]. In order to get the temperature of the steel and concrete, advanced finite element simulation is needed. In this study, heat transfer analysis was performed and verified against experimental data (see Figure 6). The results of the heat transfer analysis were used to get the temperatures for different concrete layers and steel sections, as shown in Figure 7.

According to EN 1994-1-2 [17], the buckling load in fire situations ($N_{fi,Rd,1}$) of the concrete-filled steel tubular columns can be calculated using Equation 6. In Equation 6, the design value of the plastic resistance to axial compression in the fire situation ($N_{fi,pl,Rd}$) is calculated by Equation 7.

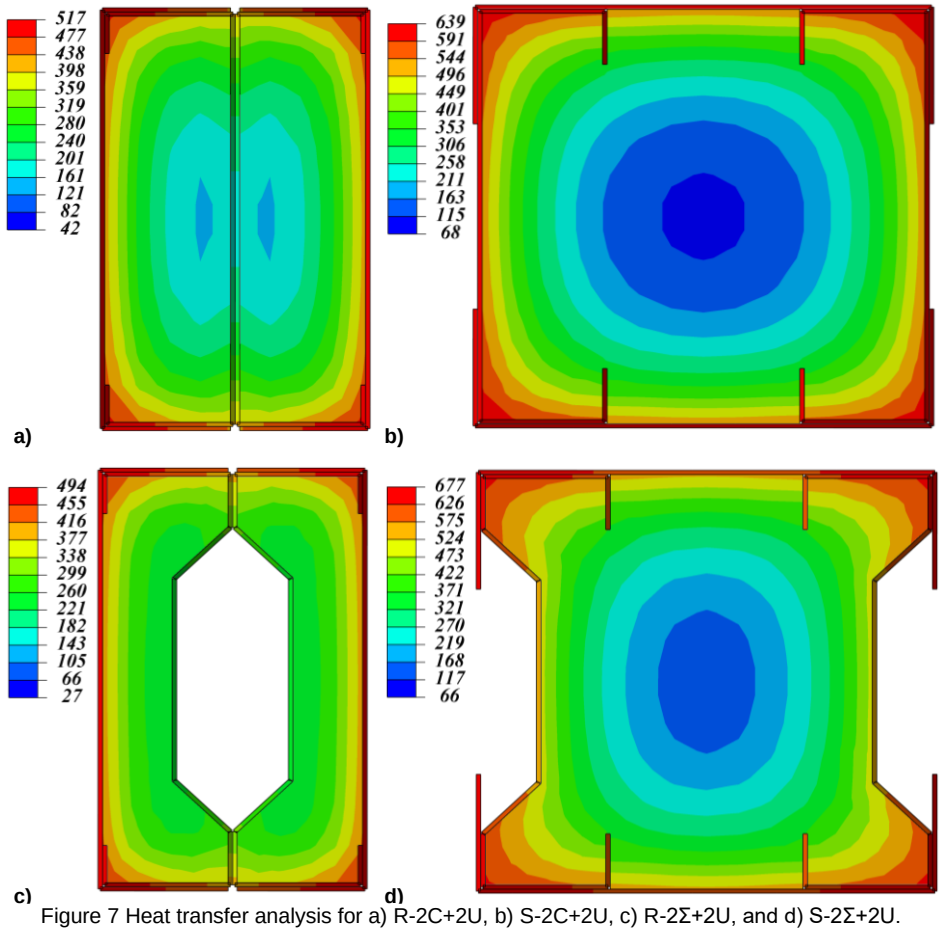

Figure 7 Heat transfer analysis for a) R-2C+2U, b) S-2C+2U, c) R-2Σ+2U, and d) S-2Σ+2U.

$$N_{fi,Rd,1} = \chi N_{fi,pl,Rd} \quad (6)$$

$$N_{fi,pl,Rd} = \sum_i {(A_{a,\theta} f_{ay,\theta})}/{\gamma_{M,fi,a}} + \sum_m {(A_{c,\theta} f_{cy,\theta})}/{\gamma_{M,fi,c}} \quad (7)$$

Moreover, the effective areas of the Class 4 cross-sections can be considered instead of the gross cross-sectional area. Therefore, another prediction ($N_{fi,\mathrm{Rd},2}$) can be based on Equation 8.

$$N_{fi,Rd,3} = \chi\left(\sum_i {\left(A_{a,eff,\theta} f_{ay,\theta}\right)}/{\gamma_{M,fi,a}} + \sum_m {\left(A_{c,\theta} f_{cy,\theta}\right)}/{\gamma_{M,fi,c}}\right) \quad (8)$$

The fire resistance of the CF-CFS built-up composite columns obtained from the tests ($P_{fi,EXP}$) was compared with those calculated from the analytical prediction ($N_{fi,Rd,1}$ and $N_{fi,Rd,2}$), as listed in Table 3. The results show that the current methodology in EN 1994-1-2 [17] over-predicts the fire resistance of such columns. However, considering the effective area for steel sections shows a proper safe and accurate prediction with an average difference of 6%. The results show that the reliability index (β) is higher than 2.5 for the analytical prediction that used an effective cross-sectional area.

Table 3 Comparing the analytical and experimental fire resistance results.

Specimen ID	$P_{fi,EXP}$ (kN)	$N_{fi,Rd,1}$ (kN)	$P_{fiEXP}/ N_{fi,Rd,1}$	$N_{fi,Rd,2}$ (kN)	$P_{fi,EXP}/ N_{b,Rd,2}$
R-2C+2U	380.56	348.44	1.09	313.40	1.21
S-2C+2U	516.85	558.99	0.92	516.90	1.00
R-2Σ+2U	330.32	342.37	0.96	317.94	1.03
S-2Σ+2U	456.98	473.82	0.96	456.39	1.00
m	-	-	0.98	-	1.06
s	-	-	0.07	-	0.1
CV (%)	-	-	7.39	-	9.6
β	-	-	2.46	-	2.63

6. Conclusions

This paper investigated the buckling and fire resistance of four concrete-filled cold-formed steel (CF-CFS) built-up columns using experimental, numerical, and analytical tools. Twenty-four experimental specimens were tested. A calibrated modeling approach was also provided for the loading at ambient and elevated temperatures. The applicability of the analytical methods of the EN 1994-1-1

[16] and EN 1994-1-2 [17] for such columns were investigated. A modification was proposed to the analytical prediction in order to be more on the safe side.
Code predictions using the effective cross-sectional area exhibit a conservative and close agreement with the buckling and fire resistance of the tested columns, as determined by comparison with values derived from EN 1994-1-1 [16] formulas. The effective cross-sectional area for the class-4 sections of the composite column provides more reliable results than those with the gross cross-sectional area, as determined by a comparison of the reliability analysis for design prediction.

7. Acknowledgments

This work is financed by national funds through the Portuguese Foundation for Science and Technology (FCT), under grant agreement 2021.06528.BD attributed to the 1st author and under the grant agreement 2020.03588. CEECIND attributed to the 2nd author.
The authors gratefully acknowledge the Portuguese Foundation for Science and Technology (FCT) for its support under the framework of the research project PTDC/ECI-EGC/31858/2017 - INNOCFSCONC - Innovative hybrid structural solutions using cold-formed steel and lightweight concrete ", financed by FEDER funds through the Competitivity Factors Operational Programme-COMPETE and by national funds through FCT, and PCIF/AGT/0062/2018 – INTERFACESEGURA – Segurança e Resiliência ao Fogo das Zonas e Interface Urbana-Florestal, financed by FCT through National funds.
This work was partly financed by FCT/MCTES through national funds (PIDDAC) under the R&D Unit Institute for Sustainability and Innovation in Structural Engineering (ISISE), under reference UIDB/04029/2020.

References

[1] N.E. Shanmugam, B. Lakshmi, State of the art report on steel–concrete composite columns, Journal of Constructional Steel Research, Volume 57, Issue 10, 2001, Pages 1041-1080, https://doi.org/10.1016/S0143-974X(01)00021-9.
[2] An He, Fangying Wang, Ou Zhao, Experimental and numerical studies of concrete-filled high-chromium stainless steel tube (CFHSST) stub columns, Thin-Walled Structures, Volume 144, 2019, 106273, https://doi.org/10.1016/j.tws.2019.106273.
[3] Ben Young, Ehab Ellobody, Experimental investigation of concrete-filled cold-formed high strength stainless steel tube columns, Journal of Constructional Steel Research, Volume 62, Issue 5, 2006, Pages 484-492, https://doi.org/10.1016/j.jcsr.2005.08.004.
[4] Dennis Lam, Leroy Gardner. (2008). Structural design of stainless steel concrete filled columns. J Constructional Steel Research, Volume 64 Issue 11 Pages 1285-1282, https://doi.org/10.1016/j.jcsr.2008.04.012
[5] Brian Uy, Zhong Tao, Lin-Hai Han. (2011). Behaviour of short and slender concrete-filled stainless steel tubular columns, Journal of Constructional Steel Research, Volume 67, Issue 3, Pages 360-378, https://doi.org/10.1016/j.jcsr.2010.10.004.
[6] Mohamed Elchalakani, M.F. Hassanein, Ali Karrech, Bo Yang, Experimental investigation of rubberised concrete-filled double skin square tubular columns under axial compression, Engineering Structures, Volume 171, 2018, Pages 730-746, https://doi.org/10.1016/j.engstruct.2018.05.123.
[7] M.A. Dabaon, M.H. El-Boghdadi, M.F. Hassanein, Experimental investigation on concrete-filled stainless steel stiffened tubular stub columns, Engineering Structures, Volume 31, Issue 2, 2009, Pages 300-307, https://doi.org/10.1016/j.engstruct.2008.08.017.
[8] Mohamed Dabaon, Saher El-Khoriby, Mahmoud El-Boghdadi, Mostafa Fahmi Hassanein, Confinement effect of stiffened and unstiffened concrete-filled stainless steel tubular stub columns, Journal of Constructional Steel Research, Volume 65, Issues 8–9, 2009, Pages 1846-1854, https://doi.org/10.1016/j.jcsr.2009.04.012.
[9] Ehab Ellobody, Ben Young, Dennis Lam, Behaviour of normal and high strength concrete-filled compact steel tube circular stub columns, Journal of Constructional Steel Research, Volume 62, Issue 7, 2006, Pages 706-715, https://doi.org/10.1016/j.jcsr.2005.11.002.
[10] Fangying Wang, Ben Young, Leroy Gardner, Compressive behaviour and design of CFDST cross-sections with stainless steel outer tubes, Journal of Constructional Steel Research, Volume 170, 2020, 105942, https://doi.org/10.1016/j.jcsr.2020.105942.
[11] Fangying Wang, Ben Young, Leroy Gardner, Compressive testing and numerical modelling of concrete-filled double skin CHS with austenitic stainless steel outer tubes, Thin-Walled Structures, Volume 141, 2019, Pages 345-359, https://doi.org/10.1016/j.tws.2019.04.003.
[12] Fangying Wang, Ben Young, Leroy Gardner, CFDST sections with square stainless steel outer tubes under axial compression: Experimental investigation, numerical modelling and design, Engineering Structures, Volume 207, 2020, 110189, https://doi.org/10.1016/j.engstruct.2020.110189.
[13] Hélder D. Craveiro, Rohola Rahnavard, Henriques, J. Rui A. Simões. Structural

Fire Performance of Concrete-Filled Built-Up Cold-Formed Steel Columns. Materials 2022, 15, 2159. https://doi.org/10.3390/ma15062159

[14] Lin-Hai Han, Feng Chen, Fei-Yu Liao, Zhong Tao, Brian Uy, Fire performance of concrete filled stainless steel tubular columns, Engineering Structures, Volume 56, 2013, Pages 165-181, https://doi.org/10.1016/j.engstruct.2013.05.005.

[15] João Paulo C. Rodrigues, Luís Laim, Behavior of Concrete-Filled Circular, Square, Rectangular, and Elliptical Hollow Columns Subjected to Fire, Journal of Structural Engineering, Volume 144, Issue 6, 2018, https://doi.org/10.1061/(ASCE)ST.1943-541X.0002035

[16] Eurocode 4. Design of composite steel and concrete structures, part 1.1: general rules and rules for building. BS EN 1994-1-1: 2004. London (UK): British Standards Institution; 2004.

[17] Design of steel and composite structures, Part 1.2: Structural fire design. ENV 1994-1-2, London, British Standards Institution: European Committee for Standardization, Eurocode 4. 2003

[18] Abaqus [61] Analysis User's Guide, Version 6.17 Dassault Systèmes Simulia USA (2017).

[19] Rohola Rahnavard, Hélder D. Craveiro, Marco Lopes, Rui A. Simões, Luís Laím, Carlos Rebelo, Concrete-filled cold-formed steel (CF-CFS) built-up columns under compression: Test and design, Thin-Walled Structures, Volume 179, 2022, 109603, https://doi.org/10.1016/j.tws.2022.109603.

[20] Rohola Rahnavard, Hélder D. Craveiro, Rui A. Simões, Luís Laím, Aldina Santiago, Buckling resistance of concrete-filled cold-formed steel (CF-CFS) built-up short columns under compression, Thin-Walled Structures, Volume 170, 2022, 108638, https://doi.org/10.1016/j.tws.2021.108638.

[21] Rohola Rahnavard, Hélder D. Craveiro, Rui A. Simões, Luís Laím, Aldina Santiago, Fire resistance of concrete-filled cold-formed steel (CF-CFS) built-up short columns, Journal of Building Engineering, Volume 48, 2022, 103854, https://doi.org/10.1016/j.jobe.2021.103854.

[22] Rohola Rahnavard, Hélder D. Craveiro, Rui A. Simões, Aldina Santiago, Equivalent temperature prediction for concrete-filled cold-formed steel (CF-CFS) built-up column sections (part A), Case Studies in Thermal Engineering, Volume 33, 2022, 101928, https://doi.org/10.1016/j.csite.2022.101928.

[23] Rohola Rahnavard, Hélder D. Craveiro, Rui A. Simões, Aldina Santiago, Equivalent temperature prediction for concrete-filled cold-formed steel (CF-CFS) built-up column sections (part B), Case Studies in Thermal Engineering, Volume 35, 2022, 102111, https://doi.org/10.1016/j.csite.2022.102111.

[24] ISO 834-1, Fire-Resistance Tests—Elements of Building Construction—Part 1: General Requirements, International Standard ISO, Geneva (1999)

[25] EN 1992-1-1 (2004) (English): Eurocode 2: Design of concrete structures - Part 1-1: General rules and rules for buildings.

[26] Hélder D. Craveiro, João Paulo C. Rodrigues, Aldina Santiago, Luís Laím, Review of the high temperature mechanical and thermal properties of the steels used in cold formed steel structures – The case of the S280 Gd+Z steel, Thin-Walled Structures, Volume 98, Part A, 2016, Pages 154-168, https://doi.org/10.1016/j.tws.2015.06.002.

[27] EN 1992-1-2 (2004) (English): Eurocode 2: Design of concrete structures - Part 1-2: General rules - Structural fire design.

[28] AISI S100-16, North American Specification for the De- sign of Cold-Formed Steel Structural Members. Wash- ington, DC, U.S.A.: AISI, 2016.

[29] Hélder D. Craveiro, Rohola Rahnavard, Luís Laím, Rui A. Simões, Aldina Santiago, Buckling behavior of closed built-up cold-formed steel columns under compression, Thin-Walled Structures, Volume 179, 2022, 109493, https://doi.org/10.1016/j.tws.2022.109493.

[30] EN 1993-1-1 (2005) (English): Eurocode 3: Design of steel structures - Part 1-1: General rules and rules for buildings

[31] EN 1993-1-3:2004, Eurocode 3: Design of steel structures, Part 1–3: General Rules, Supplementary Rules for Cold-formed Members and Sheeting, European Committee For Standardization, Brussels, Belgium, p.125.